High Resolution Diffraction Imaging of Small Scale Fractures in Shale and Carbonate Reservoirs

*Alexander Mihai Popovici (Z-Terra), Ioan Sturzu (Z-Terra), Tijmen Jan Moser (MGS & Z-Terra)

This paper was prepared for presentation during the 14th International Congress of the Brazilian Geophysical Society held in Rio de Janeiro, Brazil, August 3-6, 2015.

Abstract

Current research in the field of seismic depth imaging has identified a new approach to image with super-resolution fractured zones, fault edges, small scale faults, pinch-outs, reef edges, channel edges, salt flanks, reflector unconformities, near surface scattering objects and in general any small scattering objects, by using **Diffraction Imaging** as a complement to the structural images produced by reflection imaging. Diffraction Imaging is the imaging of discontinuities in the earth. Diffractions are the seismic response of small elements (or diffractors) in the subsurface of the earth, such as small scale faults, fractures, near surface scattering objects and in general all objects which are small compared to the wavelength of seismic waves. We show results in different areas of the world, in fractured carbonate and unconventional shale reservoirs. Using Diffraction Imaging to identify areas with increased natural fracture density, which correlate with increased production, the reservoir engineers can design an optimal well placement program that targets the sweet spots and minimizes the total number of wells used for a prospective area.

Introduction

Diffraction Imaging is a novel high-resolution imaging technology designed to image and identify in very fine detail the small scale fractures in shale and carbonate reservoirs that form areas of increased natural fracture density. These areas may be associated with higher production wells (Schoepp et. al., 2015). Diffractions are the seismic response of small elements (or diffractors) in the subsurface of the earth, such as small scale faults, fractures, near surface scattering objects and in general all objects which are small compared to the wavelength of seismic waves.

Standard approaches to obtain high-resolution information, such as coherency analysis and structure-oriented filters, derive attributes from stacked, migrated images. Diffraction imaging in comparison, acts on the pre-stack data, and has the potential to focus super-resolution structural information. Diffraction images can be used as a complement to the structural images produced by conventional reflection imaging techniques, by emphasizing small-scale structural elements that are difficult to interpret on a conventional depth image.

We show that operating in a migration framework on pre-stack data, using procedures which complement those used to enhance specular reflections, allows us to obtain higher resolution information, which is lost in conventional procedures. An efficient way to obtain diffraction images is to first separate the migration events according to the value of specularity angle, in a similar way to offset gathers; diffraction images are produced subsequently using post-processing procedures. The high-resolution potential is demonstrated by several case histories in carbonate reservoirs and unconventional shale like Eagle Ford, which show much more detail than conventional depth migration or coherence.

In 2000, shale gas represented just 1 percent of American natural gas supplies. Today, it is 40 percent and the percentage keeps increasing. The technology to drill and fracture shale formations is now exported from the USA to the rest of the world, increasing national oil and gas reserves in many other countries. Currently, there is a high level of activity for both shale gas and liquids production. Productivity in the shale plays depends on many factors including total organic content, the susceptibility of the reservoir to hydraulic fracturing and factors in the well design and completion processes. However, since reservoir porosity is exclusively fracture porosity, the detection of naturally occurring faults and fractures and the interaction of these with the hydraulic fracturing process are key areas of investigation. New high-resolution technologies are now used to visualize the structure and the natural fracture distribution and orientation in thin shale layers.

The pre-salt carbonates offshore Brazil are a potential area of application of Diffraction Imaging technology. Diffraction imaging is a direct method for the detection of subsurface discontinuities, such as small scale fractures in carbonates. The diffraction imaging is the direct response to subsurface discontinuities and is in most cases obtained from pre-stack, pre-migration data rather than post-stack, post-migration images. The diffractions volume can be used as a complement to the structural images produced by reflection imaging (Khaidukov, Landa and Moser, 2004; Taner, Fomel and Landa, 2006; Moser and Howard, 2008; Koren, Ravve and Levy, 2010; Dell and Gajewski, 2011; Moser, 2011).

Method

Diffractions are the seismic response of small elements (or diffractors) in the subsurface of the earth, such as small scale faults, near surface scattering objects and in general all objects which are small compared to the wavelength of seismic waves. Diffraction imaging is simply the process of using diffractions to determine the

locations of the small subsurface elements that produced them. Since diffractors are, by definition, smaller than the wavelength of seismic waves, diffraction imaging provides super-resolution information, which consists of image details that are beyond the classical Rayleigh limit of half a seismic wavelength. The importance of diffractions in high-resolution structural imaging has been emphasized in many recent publications (Shtivelman and Keydar 2004, Tanner et al. 2006, Fomel et al. 2006, Khaidukov et al. 2004, Moser and Howard 2008, Moser 2009, Popovici et al., 2013), however, diffraction imaging is still not a widely used tool in seismic interpretation. In fact, most of the algorithms that are used to process seismic data enhance reflections and suppress diffracted energy. The goal of diffraction imaging is not to replace these traditional algorithms, but rather to provide interpreters with an additional image to fill in the small, but potentially crucial, structural details.

An important point to note is that a true diffraction image is not optimally obtained by post-processing of a traditional seismic image, even if the seismic image is obtained by an algorithm that does not suppress diffractions. While diffractors will appear in the image, usually in the form of discontinuities, they have much lower amplitudes than reflecting structures. By imaging diffractors using the pre-stack data, the diffractor amplitude can be enhanced while the specular reflections can be attenuated. Furthermore, and more importantly, discontinuities in the seismic image can appear for a variety of reasons other than diffractions, including small errors in the velocity model of the earth that was used to obtain the image.

Several techniques for diffraction imaging have been proposed (Khaidukov et al. 2004, Tanner et al. 2006, Moser and Howard 2008, Moser 2009). They fall into two categories. In the first category are methods that separate the seismic data into two parts, one that contains the wave energy from reflections and the other that contains the wave energy from diffractions. Each component is used to provide an image through traditional seismic imaging methods. We have to keep in mind that there is no clear distinction between “reflection waves” and “diffraction waves.” By Huygens’ principle a reflector can be represented by a series of point diffractors that are positioned on its surface. In the second category are methods that do not separate the input seismic data, but rather use a different image forming technique that suppresses reflecting surfaces in the image (Moser and Howard 2008, Moser 2009). We will focus on the second category of methods, specifically on the method of Moser and Howard, which can be expressed as a reflection suppressing kernel for Kirchhoff migration.

Kirchhoff Migration

A conventional full wave Kirchhoff migration forms a seismic image as

$$V_{kirch}(x) = \sum_{s,r} \int U(t,s,r)\delta(t - t_d(s,x,r))dt$$

where, δ is the Dirac delta function, the sum is over all source and receiver pairs (s,r), U(t,s,r) is the seismic data and $t_d(s,x,r)$ is the stacking traveltime trajectory given by the traveltime from the source to the image point x and back to the receiver, $t_d(s,x,r) = T(s,x)+T(x,r)$. For a sufficiently dense grid covering the source-receiver acquisition, the traveltimes T(s,x) and T(x,r) are pre-computed by ray tracing in the velocity model, and stored on disk as travel-time tables for subsequent use in forming the image.

Kirchhoff Diffraction Imaging

The idea behind Kirchhoff diffraction imaging is to modify the image to be given by

$$W_{kirch}(x) = \sum_{s,r} \int w(s,x,r)U(t,s,r)\delta(t - t_d(s,x,r))dt$$

here all of the quantities are the same as before, except for the addition of the weight function w(s,x,r). This weight is used to suppress reflections and is obtained by the following steps. First, using standard Kirchhoff migration we find the seismic image $V_{kirch}(x)$. This image will include both reflections and diffractions, but as mentioned before, the reflections are the most dominant part of the image. The second step is to analyze the structures in the Kirchhoff image and determine the normal vector $\hat{n}(x)$ to these structures at each image point x. With this information we define the weight function by

$$w(s,x,r) = 1 - \left|\frac{\hat{n}\cdot(p^s+p^r)}{\|p^s+p^r\|}\right|,$$

where $p^s(x) = \nabla_x T(s,x)$ and $p^r(x) = \nabla_x T(x,r)$ are the gradients of the traveltimes from the source to the image point and from the image point to the receiver respectively. The logic behind this weight function is that the vector $(p^s + p^r)/\| p^s + p^r \|$ is aligned with the direction of wave propagation.

At a reflector, the wave direction is collinear with the normal vector to the reflector, thus the weight function will be nearly zero. At a diffraction point, since the seismic waves propagate in all directions, the weight function will not be zero, at least for a large part of the wave propagation directions.

An important point to note is that a true diffraction image is not optimally obtained by post-processing of a traditional seismic image, even if the seismic image is obtained by an algorithm that does not suppress diffractions. While diffractors will appear in the image, usually in the form of discontinuities, they have much lower amplitudes than reflecting structures. By imaging diffractors using the pre-stack data, the diffractor amplitude can be enhanced while the specular reflections can be attenuated. Furthermore, discontinuities in the seismic image can appear for a variety of reasons other than diffractions, including small errors in the velocity model of the earth that was used to obtain the image.

Since diffractors are, by definition, smaller than the wavelength of seismic waves, diffraction imaging provides super-resolution information. In Figure 1, we illustrate the difference between the conventional specular reflection and the higher resolution diffraction imaging. The Fresnel zone is depicted by the hatched area.

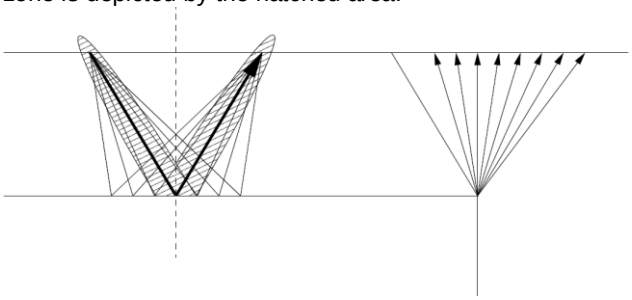

Figure 1: Comparison between a pure specular reflection and a pure diffraction case. The Fresnel zone for the reflection is depicted by the hatched area. The diffractions offer higher resolution details of discontinuities, such as the natural fractures occurring in rocks.

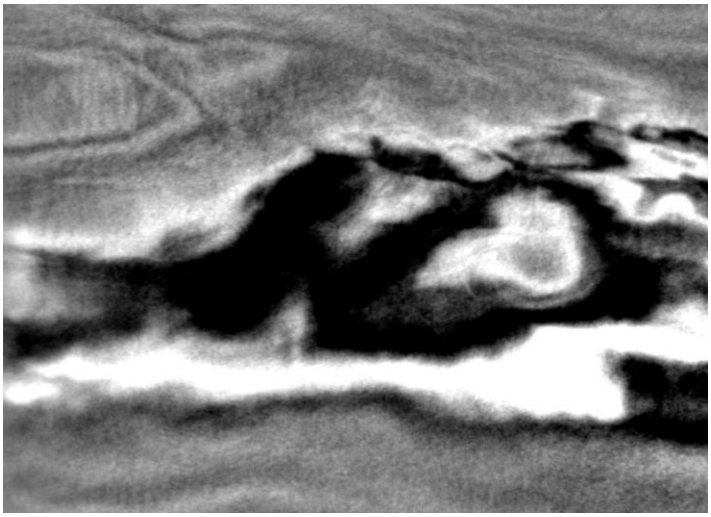

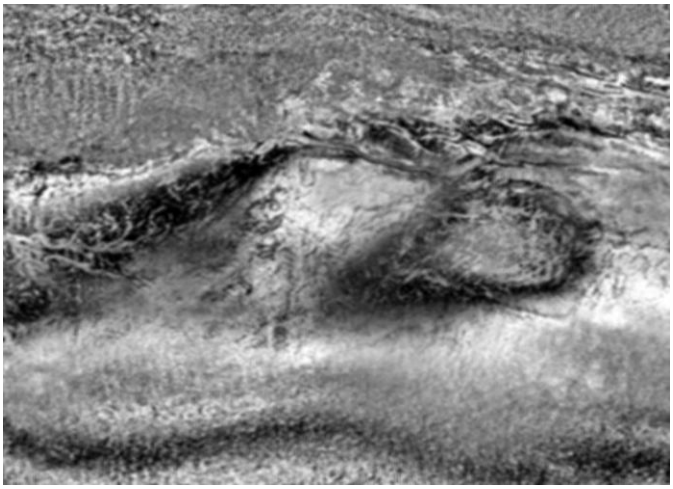

Figure 2: Comparison between a Kirchhoff PSDM depth slice and a Diffraction Imaging (DI) depth slice. The DI slice shows higher resolution details of discontinuities. *Data courtesy of Seitel*.

The main goal of conventional time and depth seismic processing is to enhance specular reflections, which follow Snell's law and for which the angle of incidence equals the reflection angle. Many time processing steps are designed to increase the lateral coherency of the reflections, from interpolation, FXY deconvolution and FK filtering, to wave-equation binning. Since diffractions have a different move-out than reflections, many processing steps designed to enhance reflections result in attenuating diffractions.

Seismic methods are generally limited in their resolving power to about one half of the dominant wavelength at the target. When the sand or shale layers are thinner than half of the wavelength, tuning and multiple-reverberation effects make the stratigraphic interpretation of the images difficult and unreliable. Decreasing the wavelength of the seismic waves reflected at the target is nearly impossible in surface seismic surveying because of the dissipative nature of the overburden that causes the attenuation of the high-frequency component of the seismic wavefield. Furthermore, the high frequencies that are present in the data are often lost during standard processing.

Specularity Gathers

A conventional full wave Kirchhoff migration forms a seismic image as a summation (stack) of the seismic events propagated to all possible locations in the subsurface. The propagation is done using travel-time tables computed in a given subsurface velocity model. The events propagated to locations which correspond to real reflections or diffractions within the subsurface, will be summed up coherently, while those propagated in locations where the velocity in the subsurface is not discontinuous will be averaged out. As for the former case, there is a quantitative difference between pure (specular) reflections and diffractions, a difference which comes from the fact that only for the specular events two close enough events will be propagated in two locations very close to each other. As a result, in the final stack, the specular events will have much higher amplitudes as compared to diffractive ones.

In the final PSDM image stack, a specular element can be approximated locally as a planar surface, with the isochron surface (computed from the exact travel-time tables) tangent to it. For diffractive events there is no such constraint. As a measure of specularity for the image of a seismic event in a location from the subsurface, one can use the departure from Snell's law, quantified as the cosine of the angle formed by the gradient of the total travel time (computed from the source of the event to the image point and further to the receiver of the event), and the normal to the local planar surface defined in that image location. Specularity is then equal to unity for pure specular events following Snell's law and smaller for diffractions, the more they disagree with Snell's law.

The technique of specularity gathers, introduced by Sturzu et al. (2013), can be used to increase both the efficiency and accuracy of the diffraction imaging technique. During the migration, partial migration output is sorted with respect to specularity angle and stored in

gathers which depend on the specularity angle. After migration the specularity taper can be efficiently designed and the specularity gathers tapered and stacked over the specularity axis, resulting in an optimal diffraction image. This is a procedure which is very similar to the familiar process of sorting partial migration output in common-image gathers, depending on offset or reflection angle, and designing a mute function to properly mute unwanted (far-offset) energy.

The use of specularity gathers has the advantage that the weighting function is designed after migration and therefore is constructed, and updated, very efficiently. In particular, the weighting function can be chosen spatially variable (w=w(x, w)), and/or can accept feedback from the geological interpretation point of view.

For a correct velocity model and in the ideal infinite-frequency limit, a specular reflection event appears in the specularity gathers as a focused spot on the Specularity axis where the specularity angle equals zero. Point diffractions appear as flat events extending the length of the axis. Edge diffractions in three dimensions appear as dipping events, as they obey Snell's law only along the edge, but not transversely to it (Moser, 2011). For finite bandwidth seismic responses, the situation is slightly different. Specular reflections also appear as dipping events, because the part of reflected energy, which falls outside the Fresnel zone, does not follow the shortest reflection path according to Fermat's principle, and is not a pure specular energy.

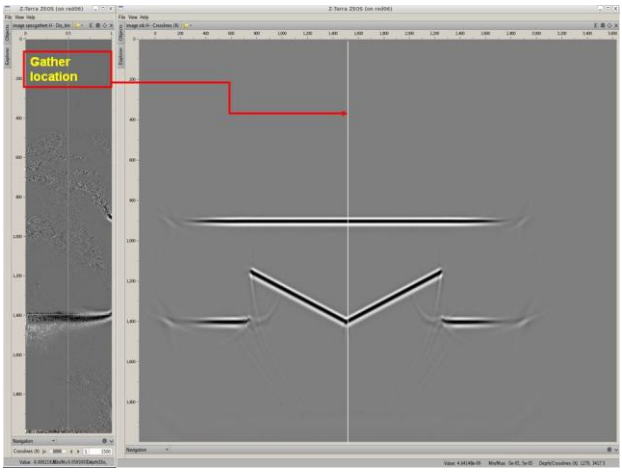

Figure 3: Specularity gather on the left and Kirchhoff PSDM depth image on the right. The energy for the specular event on the top is focused along specularity angle equal to zero. For the diffraction below the energy is distributed along the specularity axis.

Results

The Eagle Ford shale, located in south-central Texas, is one of the most prolific regions for shale liquid production. A wide range of fluids is present in the Eagle Ford play, including oil, wet gas, condensate and dry gas. As noted by previous workers, the heterogeneity of the play presents a number of exploration and production challenges (Treadgold, McLain and Sinclair, 2011; Royer and Peebles, 2012).

As shown in Figure 4, the Eagle Ford Shale overlies the Buda Limestone and is divided into two units: the Upper Eagle Ford and Lower Eagle Ford. Here we can observe the high reflectivity package which includes the Eagle Ford, the overlying Austin Chalk and the underlying Buda limestone. The overburden, although faulted, is not highly structured. An internal carbonate marker, the Kamp Ranch Member, separates the two and may be identified in wireline log signatures. In general, the lowermost Eagle Ford is characterized by high organic content (4-7% TOC) and moderate porosity (7-15%) (Treadgold, McLain and Sinclair, 2011). By contrast, the Upper Eagle Ford is significantly more calcareous and less organic rich (2-5% TOC). Total thickness of the Eagle Ford in south Texas ranges from 50 to 250 ft. The upper and lower contacts are marked by unconformities with the Buda Limestone and Austin Chalk, respectively.

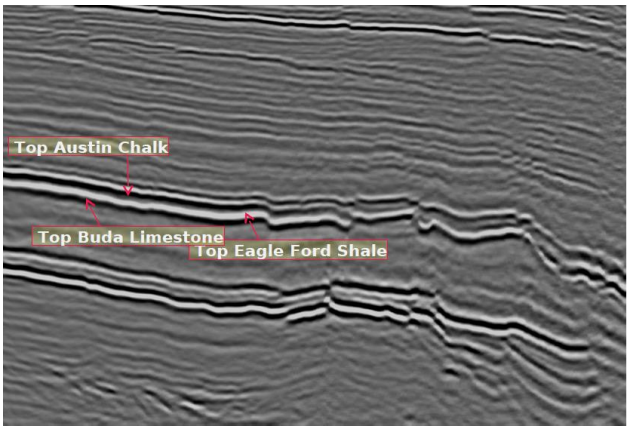

Figure 4: Eagle Ford Horizons on standard pre-stack depth migration image.

Rock properties vary significantly between the Buda, Eagle Ford and Austin Chalk, and regional 3D seismic analysis has proven effective for exploration (Yu, van Gisbergen, Dwan, Hackbarth, Shi and Lambrecht, 2013; Treadgold, McLain and Sinclair, 2011). Predicting production, however, is more complex due to small-scale variations in organic content and pre-existing fracture networks. In general, previous workers have tried to characterize heterogeneity and fractures at two scales of observation. The 'large scale' approach makes use of reflection seismic for edge detection, using attributes like curvature to define features in the Eagle Ford Formation. At the other end of the spectrum, 'fine scale' approaches attempt to bring out subseismic fractures, e.g. measuring seismic anisotropy using equivalent medium theory.

The depth slices in Figure 5 compare the diffraction image with both the standard depth migration image and a coherence cube, extracted from the depth image. The diffraction images consistently show much higher resolution detail than either the standard depth migration or the associated coherence.

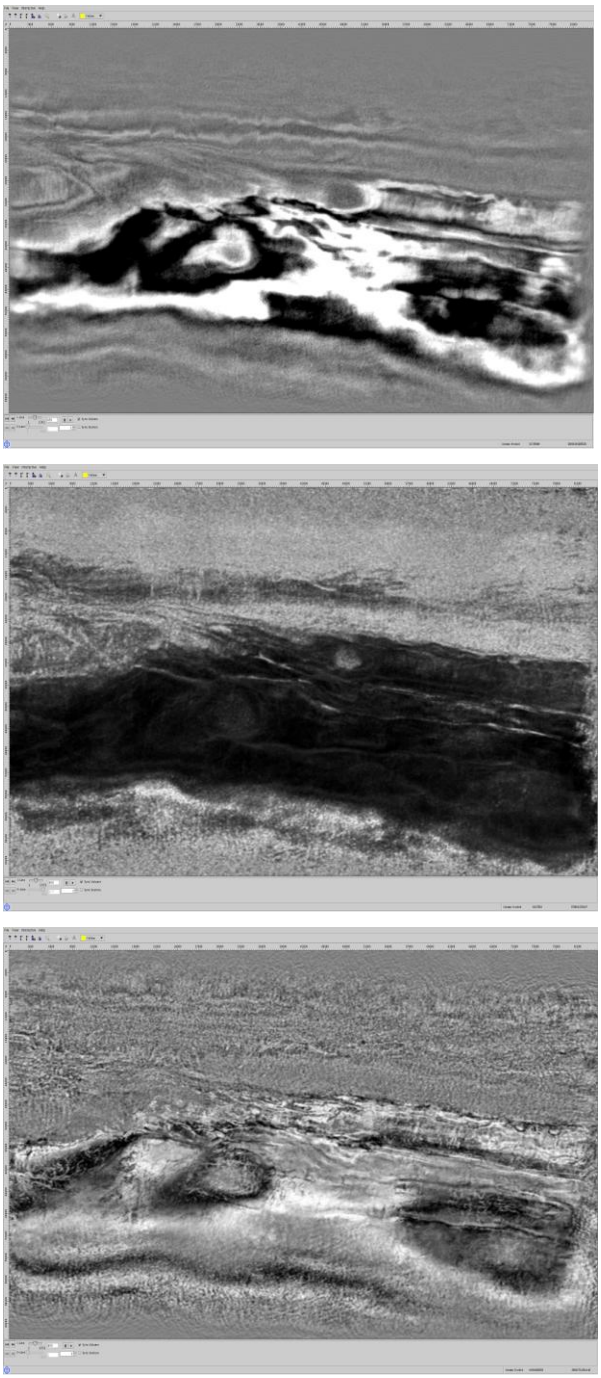

Figure 5: Depth slices over Eagle Ford at 4115m (13500ft). (Top) standard depth migration, (middle) coherence, (bottom) diffraction image.

Small-scale faulting

If we examine the spatial distribution of the diffraction response relative to the major faults, we note that the diffractivity tends to be organized in north-east south-west trending bands running parallel to the major fault trends. We interpret the area of high diffractivity to be small-scale faults or fractures antithetic to the major faults. These features occur at the seismic scale but are too small to be observed on the conventional reflection seismic. Moreover, the dense diffraction distribution could be associated with an even finer scale of faulting and fracturing not detectable via the seismic method, beyond the resolution of surface seismic data.

Conclusions

We discuss the implementation in image domain of Diffraction Imaging, a method of imaging discontinuities in the earth like fractured zones, fault edges, small scale faults, pinch-outs, reef edges, channel edges, salt flanks, reflector unconformities, near surface scattering objects and in general any small scattering objects.

We use Diffraction Imaging as a complement to the structural images produced by reflection imaging. Diffractions are the seismic response of small elements in the subsurface of the earth, objects which are small compared to the wavelength of seismic waves. We show results in different areas of the world, in fractured carbonate and unconventional shale reservoirs.

Acknowledgments

We thank Seitel for permission to show the Eagle Ford data.

References

Dell S. and Gajewski, D., 2011, Common-reflection-surface-based workflow for diffraction imaging. Geophysics, 76, S187-S195.

Fomel, S., 2002, Applications of plane-wave destruction filters: Geophysics, 67, 1946–1960.

Fomel, S., E. Landa, and M. Taner, 2006, Poststack velocity analysis by separation and imaging of seismic diffractions, in SEG Technical Program Expanded Abstracts 2006: SEG, 514, 2559–2563a.

Gelius, L.J., and Asgedom, E., 2011, Diffraction-limited imaging and beyond – the concept of super-resolution, Geophysical Prospecting, 59, 400-421.

Hentz T.F. and Ruppel C., 2010, Regional lithostratigraphy of the Eagle Ford Shale: Maverick Basin to East Texas Basin. Gulf Coast Association of Geological Societies Transactions, 60, 325-337.

Khaidukov, V., E. Landa, and T. J. Moser, 2004, Diffraction imaging by focusing-defocusing: An outlook on seismic super resolution: Geophysics, 69, 1478–1490.

Klokov, A., R. Baina, E. Landa, P. Thore, and I. Tarrass, 2010, Diffraction imaging for fracture detection: synthetic case study, in SEG Technical Program Expanded Abstracts 2010: SEG, 656,3354–3358.

Klokov, A., Baina, R. and Landa, E., 2011. Point and Edge Diffractions in Three Dimensions. 73rd EAGE Conference & Exhibition, Vienna 2011: B023.

Klokov, A., and S. Fomel, 2012, Separation and imaging of seismic diffractions using migrated dip-angle gathers: Geophysics, 77, S131–S143.

Koren, Z., and I. Ravve, 2011, Full-azimuth subsurface angle domain wavefield decomposition and imaging part

1: Directional and reflection image gathers: Geophysics, 76, S1–S13.

Koren Z., Ravve I. and Levy R., 2010, Specular-diffraction Imaging by Directional Angle Decomposition. 72nd EAGE Conference Barcelona, Extended Abstracts.

Landa, E., S. Fomel, and M. Reshef, 2008, Separation, imaging, and velocity analysis of seismic diffractions using migrated dip-angle gathers, in SEG Technical Program Expanded Abstracts 14 2008: SEG, 27, 2176–2180.

Moser T.J. and Howard C.B., 2008, Diffraction imaging in depth. Geophysical Prospecting, 56, 627-641.

Moser, T. J., 2009, Diffraction imaging in subsalt geometries and a new look at the scope of reflectivity, in EAGE Subsalt Imaging Workshop: Focus on Azimuth, Cairo, Egypt, Expanded Abstracts: EAGE.

Moser, T.J., 2010, Review of ray-Born forward modeling for migration: EAGE Conference, Extended Abstracts, G035.

Moser T.J., 2011, Edge and Tip Diffraction Imaging in Three Dimensions. 73rd EAGE Conference Vienna, Extended Abstracts.

Moser, T.J., 2012, Review of ray-Born forward modeling for migration and diffraction analysis: Studia Geophysica et Geodaetica, 56, 411-432.

Popovici, A., T. Moser, and I. Sturzu, 2014, Diffraction imaging delineates small-scale natural fractures: American Oil and Gas Reporter, 57, 89–93.

Royer T. and Peebles R., 2012, Predicting productivity in the Eagle Ford through the integration of seismic, geologic and engineering attributes. 74th EAGE Conference Copenhagen, Extended Abstracts.

Schoepp, A., Labonte, S., Landa, E., 2015, Multifocusing 3D diffraction imaging for detection of fractured zones in mudstone reservoirs: case history: Interpretation (accepted for publication, February 2015).

Shtivelman V. and Keydar S., 2005, Imaging shallow subsurface inhomogeneities by 3D multipath diffraction summation. First Break, 23, 39-42.

Sturzu I., Popovici A.M., Tanushev N., Musat I., Pelissier M.A. and Moser T.J., 2013, Specularity Gathers for Diffraction Imaging, EAGE Expanded Abstracts London, Extended Abstracts.

Sturzu, I., A. M. Popovici, and T. J. Moser, 2014, Diffraction imaging using specularity gathers: Journal of Seismic Exploration, 23, 1–18.

Sturzu, I., Popovici, A. M., Pelissier, M. A., Wolak, J. M., and Moser, T. J., 2014, Diffraction Imaging of the Eagle Ford Shale, First Break 32, November 2014.

Sturzu, I., Popovici, A. M., Moser, T. J., and Sudhakar, S., 2015, Diffraction Imaging for Well Placement Optimization in Fractured Carbonates and Unconventional Shales: Interpretation (accepted for publication, February 2015).

Taner M.T., Fomel S. and Landa E., 2006, Separation and imaging of seismic diffractions using plane wave decomposition. 76th SEG meeting New Orleans, Expanded Abstracts.

Treadgold G., Campbell B., McLain B., Sinclair S. and Nicklin D., 2011, Eagle Ford shale prospecting with 3D seismic data within a tectonic and depositional system framework. The Leading Edge, 30, 48-53.

Yu J., van Gisbergen S., Dwan S.F., Yuan R., Hackbarth C., Shi S., and Lambrecht J., 2013, Technologies unlocking unconventional gas resources – Field case studies from North America and China. 2013 International Petroleum Technology Conference Beijing, Expanded Abstracts.